color reaction: (i) the absence of serum, protein A fractions, or monoclonal IgM, (ii) substitution of anti-human IgM–HRP with HRP-conjugated antibody to mouse IgM, and (iii) the absence of gp120 (secondary and tertiary antibodies did not bind to the ELISA plate in the absence of carbonate-bicarbonate buffer). The following additional experiments ruled out artifactual binding due to ELISA conditions: (i) an immuno-dot blot assay in which the blotting of gp120 onto nitrocellulose and the subsequent Ig-binding reaction were each done at neutral pH, and (ii) the HEA-gp120 K_d determination [see (*23*)] demonstrated liquid-phase binding of antibody and antigen. In addition, because this gp120 preparation was a highly pure, native conformation product (Chiron lot MGC022; >90% by SDS–polyacrylamide gel electrophoresis gel scan, 100% binding to soluble CD4), the high-avidity competition indicates that this V_H3 IgM binds to gp120 in its native conformation. In this context, binding to nonglycosylated gp120 suggests that V_H3 IgM recognizes epitopes present on both native and denatured gp120.

18. Normal serum samples from HIV seronegative individuals were obtained from the University of California, Los Angeles (UCLA) blood donor facility. Six different serum samples tested displayed similar gp120-binding activity in our assay conditions. Monoclonal IgM samples from patients with Waldenstrom's macroglobulinemia were negative for IgG-specific HIV reactivity as tested by the UCLA Center for Health Sciences Clinical Laboratory.
19. E. H. Sasso, G. J. Silverman, M. Mannik, *J. Immunol.* **142**, 2778 (1989); *ibid.* **147**, 1877 (1991).
20. We removed IgG from normal, HIV seronegative serum with a Quik-Sep IgM protein G affinity resin kit (a gift from Isolab Inc.). Serum depleted of IgG was separated into protein A–binding and –nonbinding fractions by a protein A affinity column (Pierce) with the following modifications to the manufacturer's procedure: the binding and elution buffers described by Sasso *et al.* were used (*19*), and samples were passed over the protein A column twice.
21. Recombinant gp120 proteins from the following HIV-1 or HIV-2 strains were tested for binding to Ig: SF2, SF2 (nonglycosylated), JRFL, JR-CSF, ST, Ba-L, and BH10 (*10*) (D. W. Brighty, M. Rosenberg, I. S. Y. Chen, M. Ivey-Hoyle, *Proc. Natl. Acad. Sci. U.S.A.* **88**, 7802 (1991); M. Ivey-Hoyle *et al.*, *ibid.* p., 512.
22. O. Axelrod *et al.*, *Blood* **77**, 1484 (1991); T. Martin, S. F. Duffy, D. A. Carson, T. J. Kipps, *J. Exp. Med.* **175**, 983 (1992).
23. B. Friguet, A. F. Chaffotte, L. Djavadi-Ohaniance, M. E. Goldberg, *J. Immunol. Methods* **77**, 305 (1985).
24. F. Rousset, E. Garcia, J. Banchereau, *J. Exp. Med.* **173**, 705 (1991); J. Banchereau, P. De Paoli, A. Vallé, E. Garcia, F. Rousset, *Science* **251**, 70 (1991); T. Defrance *et al.*, *Eur. J. Immunol.* **22**, 2831 (1992); E. A. Clark and J. A. Ledbetter, *Proc. Natl. Acad. Sci. U.S.A.* **83**, 4494 (1986).
25. P. Marrack and J. Kappler, *Science* **248**, 705 (1990).
26. V. Pascual and J. D. Capra, *Curr. Biol.* 1, 315 (1991).
27. P. M. Kirkham, F. Mortari, J. A. Newton, H. W. Schroeder, *EMBO J.* 11, 603 (1992).
28. P. Casali and A. L. Notkins, *Immunol. Today* **10**, 364 (1989).
29. A. Amadori and L. Chieco-Bianchi, *ibid.* 11, 374 (1990); A. Shirai, M. Cosentino, S. F. Leitman-Klinman, D. M. Klinman, *J. Clin. Invest.* **89**, 561 (1992).
30. N. L. Haigwood *et al.*, *Vaccines 90* (Cold Spring Harbor Laboratory, Cold Spring Harbor, NY, 1990), p. 313.
31. We thank G. Higgins and his colleagues (Kaiser-Permanente Hospital, Panorama City, CA) for tonsil specimens; L. Calhoun for blood bank serum specimens; I. Chen (UCLA AIDS Institute), K. Steimer, and N. Haigwood (Chiron Corporation) for gifts of gp120 proteins; R. Jefferis, R. Schwartz, and L. Jefferies for gifts of anti-idiotypic monoclonal antibodies; K. Moore (DNAX Research Institute) for providing CDw32 L cells; E. Clark for the gift of the monoclonal anti-CD40 G28-5; the staff of the Jonsson Comprehensive Cancer Center flow cytometry core facility; Cellular Products Inc. for the Retro-tek HIV-1 ELISA kit; and S. Morrison, O. Witte, I. Chen, L. Baum, and A. Saxon for advice and critical review of this manuscript. Supported by the Jonsson Comprehensive Cancer Center, NIH grants CA12800 (J.B.) and AI28697 (Center for AIDS Research), UCLA Training Program in Biotechnology GM08375 (L.B.), American Cancer Society Fellowship PF3767 (L.G.), and the AIDS Research and Reference Reagent Program of NIH.

12 May 1993; accepted 27 July 1993

IRS-1: Essential for Insulin- and IL-4–Stimulated Mitogenesis in Hematopoietic Cells

Ling-Mei Wang, Martin G. Myers, Jr., Xiao-Jian Sun, Stuart A. Aaronson, Morris White, Jacalyn H. Pierce*

Although several interleukin-3 (IL-3)–dependent cell lines proliferate in response to IL-4 or insulin, the 32D line does not. Insulin and IL-4 sensitivity was restored to 32D cells by expression of IRS-1, the principal substrate of the insulin receptor. Although 32D cells possessed receptors for both factors, they lacked the IRS-1–related protein, 4PS, which becomes phosphorylated by tyrosine in insulin- or IL-4–responsive lines after stimulation. These results indicate that factors that bind unrelated receptors can use similar mitogenic signaling pathways in hematopoietic cells and that 4PS and IRS-1 are functionally similar proteins that are essential for insulin- and IL-4–induced proliferation.

Insulin receptor substrate–1 (IRS-1) is a hydrophilic protein that undergoes tyrosine phosphorylation immediately after insulin stimulation (*1*). It contains 20 phosphorylation sites for tyrosine and 30 for threonine and serine but possesses no apparent identity with other known proteins (*2, 3*). Tyrosine-phosphorylated sites within IRS-1 associate with high affinity to cellular proteins that contain Src homology 2 (SH2) domains, including phosphatidylinositol (PI)-3 kinase, growth factor receptor–bound protein 2 (GRB2) (Sem-5), and SH2-containing protein tyrosine phosphatase-2 (SH-PTP2) (*2, 4–6*). PI-3 kinase is activated when the SH2 domains in its 85-kD regulatory subunit (p85α) bind to tyrosine-phosphorylated IRS-1 (*7, 8*). Overexpression of IRS-1 in CHO cells enhances insulin- and insulin-like growth factor (IGF-1)–stimulated mitogenesis, and microinjection of recombinant IRS-1 into *Xenopus* oocytes mediates insulin-stimulated oocyte maturation (*9*). Insulin receptor mutants that are defective for mitogenic signaling are also incapable of inducing IRS-1 phosphorylation (*2, 10*). Although these studies imply that IRS-1 is a component of the insulin signaling pathway, they do not provide direct evidence that expression of this protein is required for insulin action.

Although the IL-3–dependent myeloid progenitor cell lines FDC-P1 and FDC-P2 do not express IRS-1, in these cells IL-4, insulin, and IGF-1 stimulate potent tyrosine phosphorylation of a protein, designated 4PS (IL-4–induced phosphotyrosine substrate) (*11, 12*). This substrate behaves like IRS-1 in that it strongly associates with p85α of PI-3 kinase after factor stimulation and migrates at 165 to 175 kD during SDS–polyacrylamide gel electrophoresis (*11, 12*). The 4PS protein is weakly recognized by a polyclonal antibody directed against IRS-1, and the phosphopeptide patterns generated by V8 digestion of the two proteins are similar but not identical (*11*). The concentrations of insulin and IL-4 required to induce mitogenesis in the FDC lines correlate with those needed to stimulate tyrosine phosphorylation of 4PS, which suggests that this IRS-1–like substrate might participate in IL-4– and insulin-mediated signal transduction in hematopoietic cells.

The 32D line has a myeloid progenitor phenotype and is IL-3–dependent like the FDC lines (*13*), but 32D cells did not proliferate upon exposure to IL-4 or insulin. Induction of DNA synthesis by IL-4 in 32D cells was negligible, and insulin had no detectable mitogenic effect at any concentration tested (Fig. 1). In contrast, IL-4 and insulin induced efficient DNA synthesis in the FDC-P2 line (Fig. 1). Receptor expression was examined by saturation binding assay: 32D cells had ~1200 IL-4 and ~500 insulin receptors per cell and FDC-P2 cells had ~1800 IL-4 and ~750 insulin receptors per cell (*14*). Because IL-4 and insulin receptor levels in 32D cells were only slightly lower than those in FDC-P2 cells, it seemed unlikely that small receptor num-

L.-M. Wang, S. A. Aaronson, J. H. Pierce, Laboratory of Cellular and Molecular Biology, National Cancer Institute, Bethesda, MD 20892.
M. G. Myers, Jr., X.-J. Sun, M. White, Joslin Diabetes Center, Department of Medicine, Harvard Medical School, Boston, MA 02215.

*To whom correspondence should be addressed.

bers were limiting the mitogenic response of 32D to IL-4 or insulin. To directly address this question, we introduced expression vectors that contained murine IL-4 receptor or human insulin receptor complementary DNAs (cDNAs) into 32D cells by electroporation (*15*). Increased receptor expression was observed when representative clonal IL-4 receptor (32D.IL-4R) and insulin receptor (32D.InsR) transfectants were compared to the parental 32D line by flow cytometric and immunoblot analysis (Fig. 2, A and B) (*16*). Saturation binding revealed that 32D.IL-4R expressed ~4600 IL-4 receptors per cell and 32D.InsR expressed ~16,000 insulin receptors per cell (*14*).

Increased expression of the IL-4 receptor in 32D.IL-4R cells allowed IL-4 to induce a weak, albeit enhanced, mitogenic response when compared to the parental line, and insulin treatment of the 32D.InsR transfectant resulted in similar low [^{3}H]thymidine incorporation (Fig. 3, A and B). In contrast to that in the FDC-P2 line, tyrosine phosphorylation of 4PS was not detected in 32D cells even after receptor overexpression (Fig. 3C). IL-4 or insulin stimulation of 32D and receptor (32D.receptor) transfectants resulted in tyrosine phosphorylation of only a few minor bands (Fig. 3C). Tyrosine phosphorylation of both the IL-4 receptor and β-subunit of the insulin receptor could be detected when factor-stimulated 32D.receptor cell lysates were immunoprecipitated with antibodies to phosphotyrosine (anti-phosphotyrosine) and subsequently immunoblotted with receptor-specific sera (*17*). Because the β-subunit of the insulin receptor is autophosphorylated in response to ligand binding and a portion of the IL-4 receptor becomes tyrosine-phosphorylated by an unknown kinase that is activated upon IL-4 stimulation (*12, 18*), these results provide evidence that both transfected receptors are functional despite their inability to efficiently mediate ligand-dependent mitogenic responses in 32D cells. Thus, a lack of 4PS or IRS-1 expression might explain the insensitivity of 32D cells to IL-4 and insulin.

Because the gene encoding 4PS has not yet been molecularly cloned, an expression vector that contained a rat IRS-1 cDNA was transfected into 32D and 32D.receptor lines (*15*). IRS-1 was highly expressed in the lines transfected with the IRS-1 vector, whereas none was detected in the 32D parental or 32D.receptor lines as determined by immunoblot analysis (*19*). Receptor expression was not altered after transfection of the 32D.receptor lines with the IRS-1 expression vector, as determined by flow cytometric analysis (*16*).

The ability of IL-4 and insulin to induce tyrosine phosphorylation of IRS-1 in the different transfectants was next examined. A prominent tyrosine-phosphorylated 170-kD band was observed when lysates from factor-stimulated 32D.IRS-1 cells or 32D.receptor.IRS-1 cells were immunoprecipitated with antiserum to IRS-1 and subsequently immunoblotted with anti-phosphotyrosine (Fig. 4A). Although some basal tyrosine phosphorylation of IRS-1 was observed in the transfectants, the amount was considerably smaller than that seen after factor stimulation. When the same lysates were both immunoprecipitated and immunoblotted with anti-phosphotyrosine, a similar pattern was observed (Fig. 4B). Phosphotyrosine-containing bands that migrated below 170 kD were unidentified and likely represent degradation products of IRS-1 (*19*).

Expression of IRS-1 in the parental 32D cells permitted IL-4 and insulin to induce a distinct mitogenic response (Fig. 4, C and D). The response of 32D.IRS-1 cells to IL-4 or insulin was greater than that of either 32D.IL-4R or 32D.InsR cells to their respective ligands. Stimulation of 32D.IL-4R.IRS-1 cells with IL-4 or 32D.InsR.IRS-1 cells with insulin led to even more efficient DNA synthesis. Whereas the 32D.IRS-1 cells did not respond as efficiently as FDC-P2 cells to insulin or IL-4, the responses of the 32D.receptor.IRS-1 transfectants to their respective ligands were comparable to those of the FDC-P2 line. Thus, IRS-1 expression appears to be crucial for IL-4– and insulin-stimulated mitogenesis in 32D cells.

The ability of the various 32D transfectants to grow continuously in medium that contained IL-4 or insulin was also analyzed (Table 1). The parental 32D and 32D.receptor transfectants could not be propagated in growth medium supplemented with

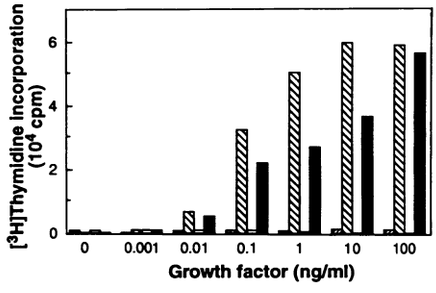

Fig. 1. Comparison of the mitogenic response induced by IL-4 or insulin in 32D and FDC-P2 cell lines. The 32D or FDC-P2 cell lines (10^5 cells per milliliter) were exposed to various concentrations of recombinant murine IL-4 or human insulin, and DNA synthesis was measured after 40 hours. [^{3}H]Thymidine (0.5 μCi/ml) was added for the last 4 hours of the incubation period, and samples were collected by an automatic cell harvester and counted by liquid scintillation as described (*11, 12*). Data points are the mean of triplicate samples and are expressed as counts per minute (cpm) of incorporated [^{3}H]thymidine. First bars, 32D + IL-4; second bars, FDC-P2 + IL-4; third bars, 32D + insulin; fourth bars, FDC-P2 + insulin.

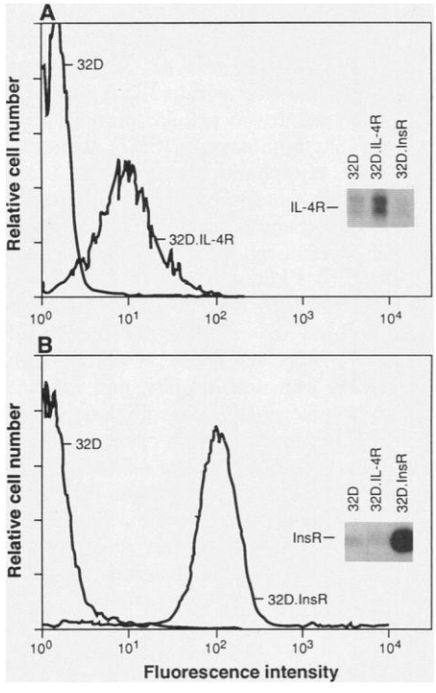

Fig. 2. Overexpression of IL-4 or insulin receptors in the 32D cell line. (**A**) Expression of murine IL-4 receptors on 32D and 32D.IL-4R cells as determined by flow cytometric and immunoblot (insert) analysis (*16*). The IL-4 receptor–specific bands migrated at 110 to 130 kD. (**B**) Expression of human insulin receptors on 32D and 32D.InsR cells as determined by flow cytometric or immunoblot (insert) analysis (*16*). The insulin receptor band specific for the β-subunit migrated at 97 kD.

Table 1. Long-term growth of 32D and various 32D transfectants in IL-4 and insulin. Exponentially growing cells were washed twice and plated (5×10^4 cells per milliliter) in RPMI 1640 medium supplemented with 10% fetal bovine serum and recombinant IL-4 (10 ng/ml) or human insulin (100 ng/ml). Cells were transferred at a split ratio of 1:10 to 1:50 biweekly. Those cell lines that continued to divide for over 2 months were scored as positive (+). Cell lines that did not survive were retested twice before being scored as negative (−). Ins., insulin.

Cell line	Growth factor			
	None	IL-4	Insulin	IL-4 and insulin
32D	−	−	−	−
32D.IL-4R	−	−	−	−
32D.InsR	−	−	−	−
32D.IRS-1	−	−	−	+
32D.IL-4R.IRS-1	−	+	−	+
32D.InsR.IRS-1	−	−	+	+

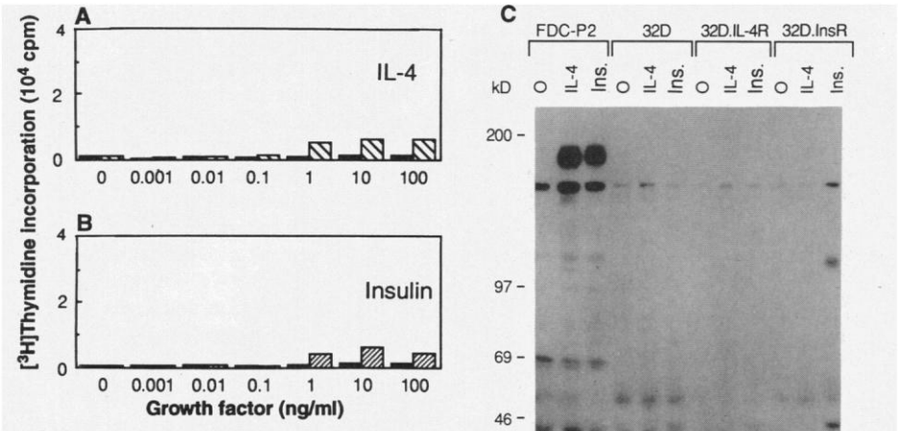

Fig. 3. Comparison of the mitogenic response and phosphotyrosine pattern induced by IL-4 or insulin in 32D (solid bars) and 32D.receptor (hatched bars) transfectants. Analysis of the mitogenic response of (**A**) 32D and 32D.IL-4R to serial dilutions of recombinant murine IL-4 or (**B**) 32D and 32D.InsR to human insulin. DNA synthesis was measured as described (Fig. 1) (*11, 12*). (**C**) The phosphotyrosine pattern induced by IL-4 or insulin in FDC-P2, 32D, and 32D.receptor transfectants was determined as described (*11, 12*). Briefly, quiescent cells were treated with IL-4 (100 ng/ml) or insulin (1 μg/ml) for 10 min and lysed. Equal amounts of protein (2 mg) from cell lysates were immunoprecipitated with anti-phosphotyrosine (UBI, Inc., Lake Placid, New York) and subsequently immunoblotted with anti-phosphotyrosine.

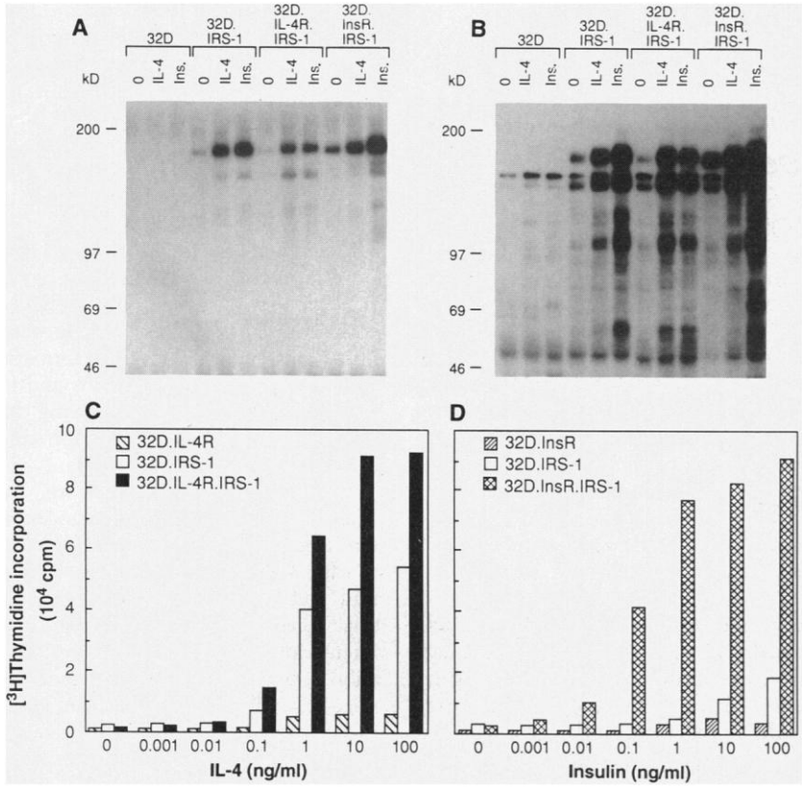

Fig. 4. Comparison of the mitogenic response and analysis of phosphotyrosine-containing proteins induced by IL-4 or insulin in the different 32D.receptor and 32D.IRS-1 transfectants. Detection of (**A**) tyrosine-phosphorylated IRS-1 induced by IL-4 or insulin in 32D, 32D.IRS-1, and 32D.receptor.IRS-1 transfectants by immunoprecipitation with an IRS-1–specific polyclonal serum followed by immunoblot analysis with anti-phosphotyrosine as described (*11*). (**B**) Detection of total tyrosine-phosphorylated proteins induced by IL-4 or insulin in the 32D, 32D.IRS-1, and 32D.receptor.IRS-1 transfectants as determined by immunoprecipitation and subsequent immunoblot analysis with anti-phosphotyrosine (*11, 12*). (**C** and **D**) Analysis of the mitogenic response of (C) 32D.IL-4R, 32D.IRS-1, and 32D.IL-4R.IRS-1 to IL-4 or (D) 32D.InsR, 32D.IRS-1, and 32D.InsR.IRS-1 to insulin as described (Fig. 1) (*11, 12*).

IL-4, insulin, or a combination of both factors. In contrast, 32D.IRS-1 cells grew indefinitely in medium that contained IL-4 and insulin. Moreover, each 32D.receptor. IRS-1 transfectant required only its corresponding ligand to sustain continued proliferation. The FDC lines, like 32D.IRS-1, can be propagated in a combination of IL-4 and insulin (*11*). Overexpression of IGF-1 receptors in the FDC-P1 line results in insulin- or IGF-1–dependent long-term growth (*20*). These results suggest that cell surface receptor numbers for IL-4 and insulin are limiting on both 32D and FDC cell lines and that dual stimulation leads to an additive signal mediated by IRS-1 or 4PS, which is sufficient to support continuous growth.

Insulin-induced tyrosine phosphorylation of IRS-1 leads to its association with the SH2-SH3–containing growth factor receptor–bound protein 2 (GRB2) protein that is thought to be linked to *ras* signaling (*5, 21*). Although insulin stimulation has been demonstrated to induce $p21^{ras}$ activation, it has been reported that IL-4 does not affect this important signaling molecule (*22*). Because the IL-4 receptor does not contain any known intrinsic tyrosine kinase domain (*23*), IL-4 binding must result in activation of an independent cellular tyrosine kinase. Therefore, it is possible that stimulation with insulin or IL-4 leads to differential tyrosine phosphorylation of IRS-1 or 4PS that, in turn, regulates their interaction with different downstream signaling elements.

The fortuitous lack of detectable IRS-1 or 4PS expression in 32D cells has allowed us to demonstrate that a specific tyrosine kinase substrate can transmit a growth factor–initiated signal by two unrelated growth factors and should provide a means to determine if differences exist in insulin and IL-4 signal transduction mediated by IRS-1. The 32D system will also allow mutational analysis of IRS-1 to delineate which regions are most important for coupling with mitogenic or metabolic signaling pathways.

REFERENCES AND NOTES

1. M. F. White, R. Maron, C. R. Kahn, *Nature* **318**, 183 (1985).
2. X.-J. Sun *et al.*, *ibid.* **352**, 73 (1991).
3. S. R. Keller, R. Aebersold, C. W. Garner, G. E. Lienhard, *Biochim. Biophys. Acta* **1172**, 323 (1993).
4. J. M. Backer, G. G. Schroeder, D. A. Cahill, A. Ullrich, M. F. White, *J. Biol. Chem.* **265**, 16450 (1990).
5. E. Y. Skolnik *et al.*, *EMBO J.* **12**, 1929 (1993).
6. R. M. Freeman, J. Plutzky, B. G. Neel, *Proc. Natl. Acad. Sci. U.S.A.* **89**, 11239 (1992).
7. J. M. Backer *et al.*, *EMBO J.* **11**, 3469 (1992).
8. M. G. Myers, Jr., *et al.*, *Proc. Natl. Acad. Sci. U.S.A.* **89**, 10350 (1992).
9. X.-J. Sun *et al.*, *J. Biol. Chem.* **267**, 22662 (1992); L.-M. Chuang *et al.*, *Proc. Natl. Acad. Sci. U.S.A.*, in press.

10. C. K. Chou *et al.*, *J. Biol. Chem.* **262**, 1842 (1987); M. F. White *et al.*, *Cell* **54**, 641 (1988); J. M. Backer *et al.*, *Biochemistry* **30**, 6366 (1991).
11. L.-M. Wang *et al.*, *Proc. Natl. Acad. Sci. U.S.A.* **90**, 4032 (1993).
12. L.-M. Wang *et al.*, *EMBO J.* **11**, 4899 (1992).
13. T. M. Dexter, J. Garland, D. Scott, E. Skolnik, D. Metcalf, *J. Exp. Med.* **152**, 1036 (1980); J. S. Greenberger *et al.*, *Fed. Proc.* **42**, 2762 (1983); G. S. Le Gros, S. Gillis, J. D. Watson, *J. Immunol.* **135**, 4009 (1985).
14. The binding of ^{125}I-labeled insulin or ^{125}I-labeled IL-4 was measured as described [J. Lowenthal *et al.*, *J. Immunol.* **140**, 456 (1988)]. Briefly, aliquots of cells were incubated at 4°C for 2 hours in the presence of labeled factor in a volume of 200 μl. Cell-bound ^{125}I-insulin or ^{125}I-IL-4 was separated from unbound factor by centrifugation through an oil gradient. Nonspecific binding was measured in the presence of 100-fold excess of unlabeled factor and subtracted from the total bound counts per minute. The mean of cell-bound counts per minute at plateau from triplicate samples was then used to determine the receptor number per cell.
15. Electroporation of 32D cells was done as described [J. H. Pierce *et al.*, *Science* **239**, 628 (1988)]. The murine IL-4 receptor cDNA was inserted into the LTR-2 expression vector containing an SV40-driven *gpt* selectable marker [P. P. Di Fiore *et al.*, *Cell* **51**, 1063 (1987)]. The human insulin receptor expression vector was cotransfected with an SV2*neo* vector. The expression vector with rat IRS-1 cDNA contains a histidinol resistance marker (*7*). Transfected populations were selected by emergence in growth medium containing 80 μM mycophenolic acid and the addition of hypoxanthine, aminopterin, thymidine (HAT), or geneticin (750 μg/ml), or 10 μM histidinol, respectively, for each protein expressed.
16. Flow cytometric analysis was done on FACScan (Becton-Dickinson San Jose, CA). The IL-4 receptor monoclonal antibody (mAb) (1 μg/ml) (Immunex Seattle, WA) and the human α-subunit insulin receptor mAb (Amersham) were used at a concentration of 1 μg/ml and a 1:100 dilution, respectively. Phycoerythrin-conjugated goat antibodies to rat or mouse (both at 1:100) from Caltag were used as secondary antibodies. Rabbit antipeptide sera specific for the IL-4 receptor (*12*) or insulin receptor (*7*) (1:500 dilutions) were used to immunoblot 300 μg of protein from cell lysates as described.
17. J. H. Pierce and L.-M. Wang, unpublished observations.
18. M. Kasuga, F. A. Karlsson, C. R. Kahn, *Science* **215**, 185 (1982).
19. J. H. Pierce, L.-M. Wang, M. G. Myers, Jr., unpublished observations.
20. J. A. McCubrey *et al.*, *Blood* **78**, 921 (1991).
21. E. J. Lowenstein *et al.*, *Cell* **70**, 431 (1992).
22. B. M. Burgering, A. J. Snyder, J. A. Massen, A. Van Eb, J. L. Bos, *Mol. Cell. Biol.* **9**, 4312 (1989); J. B. Gibbs, M. S. Marshall, E. M. Skolnik, R. A. Dixon, U. S. Vogel, *J. Biol. Chem.* **265**, 20437 (1990); T. Satoh, M. Nakafuku, A. Miyajima, Y. Kajiro, *Proc. Natl. Acad. Sci. U.S.A.* **88**, 3314 (1991); V. Duronio, M. J. Welham, S. Abraham, P. Dryden, J. W. Schrader, *ibid.* **89**, 1587 (1992).
23. B. Mosley *et al.*, *Cell* **59**, 335 (1989); J.-P. Galizzi *et al.*, *Int. Immunol.* **2**, 669 (1990).
24. We thank C. Knicley and F. Liu for excellent technical assistance; P. Beckmann, Immunex Corporation, for providing reagents; and W. Paul and A. Keegan for discussions. Supported in part by NIH grant DK-43808.

15 April 1993; accepted 22 July 1993

Neuroblast Specification and Formation Regulated by *wingless* in the *Drosophila* CNS

Quynh Chu-LaGraff and Chris Q. Doe*

The *Drosophila* central nervous system (CNS) develops from a heterogeneous population of neural stem cells (neuroblasts), yet the genes regulating neuroblast determination remain unknown. The segmentation gene *wingless* is regionally expressed in the neuroectoderm from which neuroblasts develop. A conditional *wingless* mutation is used to inactivate CNS function without affecting segmentation. The stripe of wingless-expressing neuroectoderm generates apparently normal neuroblasts after wingless inactivation; however, adjacent anterior and posterior neuroectoderm requires wingless nonautonomously for subsequent neuroblast determination and formation. Loss of wingless results in the absence or duplication of identified neuroblasts, highlighting its role in generating neuroblast diversity in the CNS.

The insect CNS is composed of hundreds of neurons, each expressing a unique combination of neurotransmitters, ion channels, receptors, and cell surface molecules. The generation of neuronal diversity begins immediately after gastrulation, when the superficial ventral cells of the embryo form a neuroectoderm. Within this neuroectoderm, individual cells enlarge and delaminate inwards to produce a stereotyped, subectodermal array of 30 unique neural precursor cells (neuroblasts; NBs) (*1*). Each NB divides according to an invariant cell lineage to generate an average of five ganglion mother cells (GMCs); subsequently, each GMC produces a characteristic pair of neurons (*2*). Genes regulating NB formation (*3–5*) and GMC and neuronal determination (*6–9*) have been identified; however, genes controlling NB determination have yet to be described.

The segment polarity class of genes are the best candidates for genes controlling NB specification (*10*). Many of these genes are regionally expressed in the neuroectoderm, and mutations often result in abnormal CNS development (*11*). One example is the *wingless* (*wg*) gene, which encodes a secreted glycoprotein that is required to specify the fate of epidermal cells (*12–14*) and is also required for the development of the *even-skipped*–expressing (eve$^+$) RP2 motoneuron in the CNS (*11*). The CNS phenotype could be due to changes in the fate of neuroectodermal cells, NBs, GMCs, the RP2 neuron, or cell death at any of these stages. Here we use a temperature-sensitive *wg* mutation and eight molecular markers that label specific subsets of neuroectodermal cells, NBs, GMCs, and neurons to determine the role of *wg* during CNS development.

The first 10 NBs form about 30 min after gastrulation [early stage 9; staging according to (*15*)]. These S1 NBs form an orthogonal array of four rows (2/3, 4, 5, 6/7) and three columns (medial, intermediate, and lateral) in each hemisegment (Fig. 1). A second phase of NB formation occurs 40 min later (mid–stage 9), when the five S2 NBs enlarge and delaminate (Fig. 1). The *wg* gene is transcribed specifically in row 5 neuroectoderm and NBs (*1*), and the secreted wg protein can be detected in the adjacent row 4 and row 6/7 neuroectoderm and NBs (*12, 14*). To determine the CNS function of *wg*, we assayed expression of our molecular markers in embryos homozygous for the temperature-sensitive wg^{IL114} mutation grown at the restrictive temperature. These embryos have an epidermal and CNS phenotype indistinguishable from that of embryos homozygous for the null wg^{CX4} allele (*16*) and will be referred to as wg$^-$ embryos.

Wild-type and wg$^-$ embryos have identical patterns of all markers in S1 NBs at early stage 9 (*17*). This result suggests that *wg* is not required for the formation or initial specification of S1 NBs and is consistent with previous data showing that loss of *wg* does not affect the formation of several identified S1 NBs (*18*).

The first CNS phenotype in wg$^-$ embryos is an alteration in the neuroectodermal pattern of runt and the enhancer trap line 5953 at early stage 9 (S1 NB stage). Changes in runt and 5953 patterns are documented in stage 10 embryos because the staining is more intense in older embryos; however, the alterations shown reflect changes seen at early stage 9. In wild-type embryos, runt is observed in neuroectoderm of row 2/3 (Fig. 1A). In wg$^-$ embryos, runt expression expands into row 4 (but not into row 5 or 6/7), indicating that *wg* nonautonomously represses runt expression specifically in row 4 neuroectoderm (Fig. 1B). In wild-type embryos, 5953 is expressed in row 2/3, in a patch of cells in row 4 (where NB 4-2 will delaminate), and in a patch of cells in row 5 (Fig. 1C). In wg$^-$ embryos, there is a selective loss of 5953 expression in row 4 (Fig. 1D), but no change

Department of Cell and Structural Biology, University of Illinois, Urbana, IL 61801.

*To whom correspondence should be addressed.